Progress In Electromagnetics Research M, Vol. 66, 65–72, 2018

Reconfigurable Cylindrical Plasma Antenna

Oumar A. Barro*, Mohammed Himdi, and Olivier Lafond

Abstract—This paper presents the performance of cylindrical plasma antenna. A plasma tube is used as radiating element. The antenna is designed and works at different frequencies. To couple electromagnetic signal from the coaxial probe to the plasma column, a coupling system is realized. It permits to excite the tube in order to have a monopole or dipole antenna. The performances of the cylindrical plasma antenna are given in terms of S_{11}, gain and radiations patterns.

1. INTRODUCTION

For many years, plasma antennas have been studied due to their ability to be conductor or transparent [1, 2]. The main advantage of using plasma antennas instead of metallic elements is that they allow electrical control rather than mechanical one. In particular, for military applications, the possibility of having conducting elements only when the useful signal needs to be transmitted makes antenna detection by hostile radars difficult.

Plasma is the fourth state of the matter. When the plasma inside a container (tube in our case) is energized (state ON), the media performs like a conductive element capable to reflect radio signal like a metal. However, when the tube is de-energized (state OFF), the plasma is non-conductor and acts as a dielectric medium. Some antennas using plasma have been studied in the literature. In [3–14], the authors proposed plasma antenna for which an ionized tube was the radiating element. In [15], the authors proposed a dipole plasma antenna with a lumped element equivalent circuit to represent the input impedance.

Hence, the aim of this paper is to present simulated and experimental results to verify the performance in terms of radiation pattern, gain, and S_{11} of the cylindrical plasma antenna with feeding system to couple electromagnetic signal from a coaxial probe to the plasma column at many frequencies. Different radiations patterns are offered by this antenna system depending on the working frequency.

The paper is organized as follows. In Section 2, we describe the modeling and simulation of the cylindrical plasma antenna with the coupling system. The comparison between simulations and measurements is presented in Section 3. A conclusion is given in Section 4.

2. MODELING AND SIMULATIONS

In this section, we describe the plasma antenna based on a fluorescent tube and its RF coupling part. The idea is to design a monopole plasma antenna. The illustration of the antenna system is shown in Fig. 1. The antenna is composed of a fluorescent lamp fed by a coaxial probe through a particular coupling system leading to the radiation of the plasma tube. The height of the commercial fluorescent lamp is 590 mm, and the tube diameter is 26 mm. A reflector of 1 m × 1 m (see Fig. 1) is placed below the antenna at a distance d from the antenna system in order to increase the gain and reduce the back radiations. Thanks to the dimensions of the existing lamps, the operating frequencies are not specifically in known frequency bands or known applications. This justifies the frequencies used in this paper.

Received 9 November 2017, Accepted 12 March 2018, Scheduled 26 March 2018

* Corresponding author: Oumar Barro (oumar-alassane.barro@univ-rennes1.fr).

The authors are with the Institute of Electronics and Telecommunications of Rennes, UMR CNRS 6164, University of Rennes 1, France.

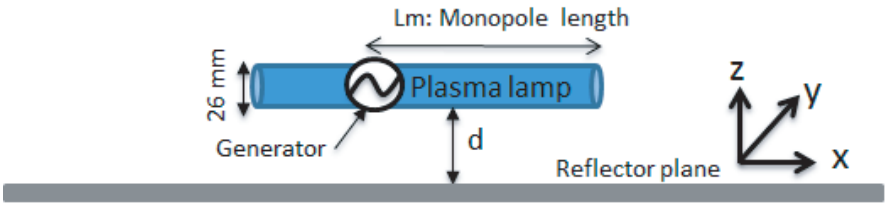

Figure 1. Monopole with reflector.

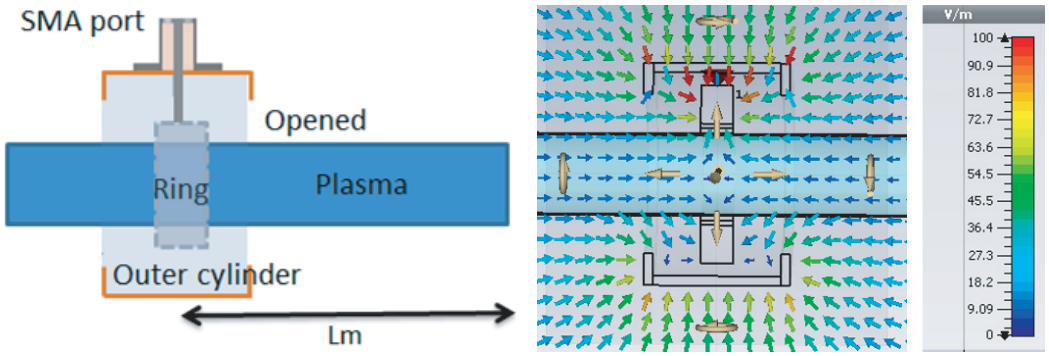

(a) (b)

Figure 2. Coupling system. (a) Symmetric cavity. (b) E-field distribution.

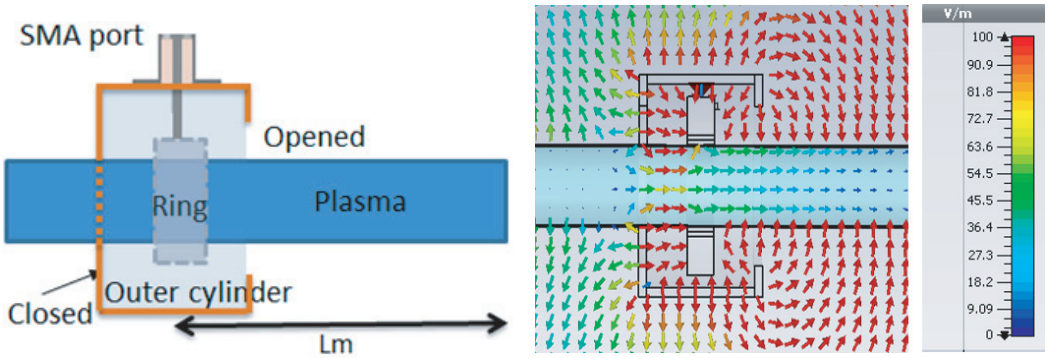

(a) (b)

Figure 3. Coupling system. (a) Dissymmetric cavity. (b) E-field distribution.

For simulations performed with CST Microwave Studio [16], the tube containing gas is made from lossy pyrex glass with $\epsilon_r = 4.82$, $\tan\delta = 0.005$ and thickness of 0.5 mm. The plasma obeys the Drude model defined by two parameters: plasma angular frequency ω_p and electron-neutral collision frequency ν. The plasma parameters used in this study are $\nu = 900$ MHz and $\omega_p = 43.9823\ 10^9$ rad/s [17].

Because the glass holding the gas, there is no physical contact between the inner coaxial line and the plasma. Therefore, a coupling system is necessary in order to induce an electromagnetic field inside the tube. Furthermore, the E-field must be parallel to the plasma tube (horizontal electromagnetic E-field). The coupling area between SMA connector and the lamp is composed by a metallic ring surrounding the plasma tube and an outer metallic cylinder (see Figs. 2(a) and 3(a)). The width of the ring is 10 mm, and this ring is shielded by an outer cylinder whose diameter and width are 70 mm and 40 mm, respectively. The inner coaxial line is connected to the ring while its ground is linked to the outer cylinder.

In the first time, two flaps with an aperture of 45 mm are placed in both sides (see Fig. 2(a)). In this coupling system, the field distribution has vertical and horizontal components, and due to the symmetry this field distribution cancels mutually (see Fig. 2(b)). Consequently, the system does not couple the plasma. In order to have a field distribution along the tube, the coupling system is dissymmetric (see Fig. 3(a)) by opening one side and closing the other. Therefore, a horizontal strong electric field is coupled to the plasma and allows the tube plasma to radiate (see Fig. 3(b)) while the vertical E-field components cancel mutually.

The realized monopole plasma antenna without reflector plane is shown in Fig. 4.

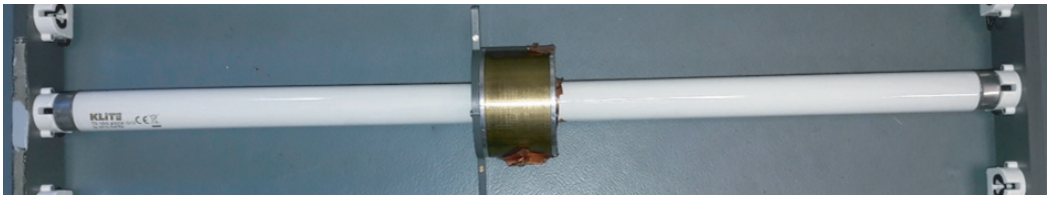

Figure 4. Realized antenna.

The main idea of this work is to design an antenna which can radiate (Plasma ON) or not (plasma OFF). In the last configuration, this antenna becomes furtive thanks to the use of plasma lamp.

3. RESULTS AND DISCUSSION

Fig. 5 presents the current distribution along the tube for different frequencies. This current distribution allow to know the length of the lamp in terms of guided wavelength ($\lambda_g/2$) and how the antenna will radiate. Between two minimums, the distance is evaluated, and this distance corresponds to $\lambda_g/2$. This system is similar to one conductor coated by a dielectric substrate [18, 19].

Fig. 5 also shows that the effective permittivities are similar and equal almost to 2 for all frequencies. At 500 and 550 MHz, the current distribution is stronger towards the opened side, but when the

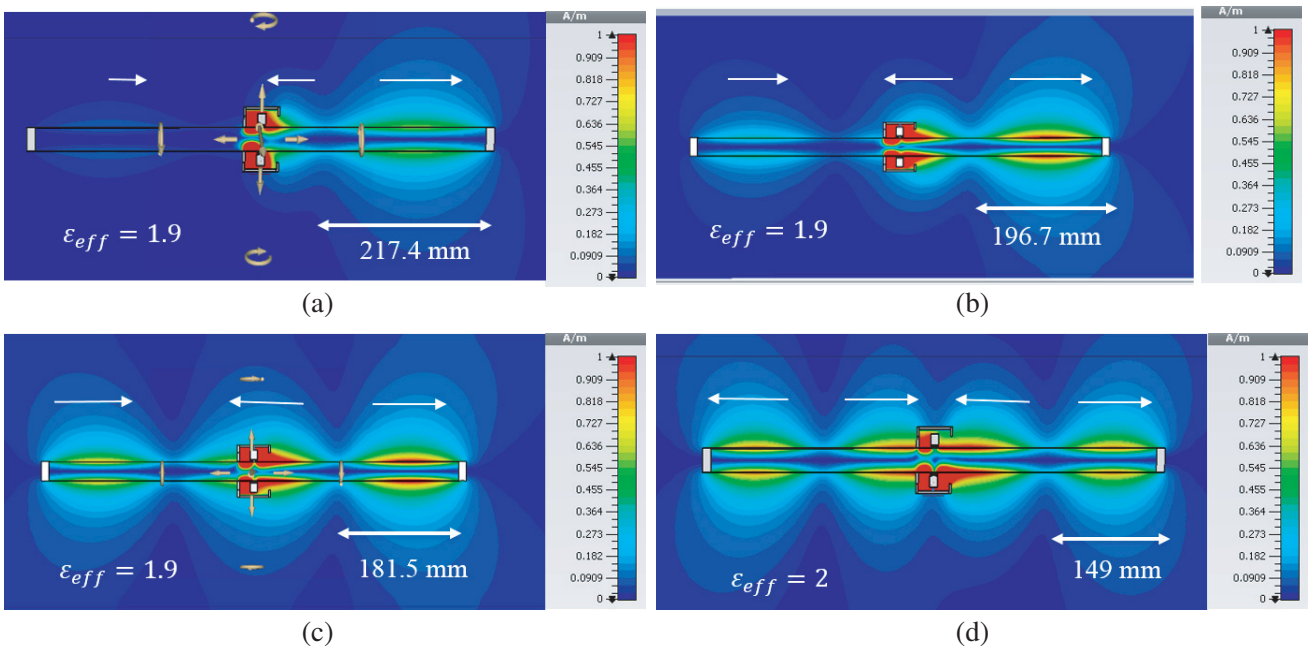

Figure 5. Current distribution for different frequencies. (a) 500 MHz. (b) 550 MHz. (c) 600 MHz. (d) 700 MHz.

frequency increases (600 and 700 MHz), the coupling system presents leakage; therefore, the current distributions are similar in the two directions. In these cases, the monopole looks like a dipole but with a simple feeding system without balun. Both cases can be used depending on the application. If we want to have dipole behavior for all frequencies, we can put two identical coupling systems side by side and use a balun in order to obtain symmetric current distribution along the tube.

The simulated and measured magnitudes of S_{11} parameters are shown in Fig. 6. The simulated and measured results are in quite good agreement. This antenna is not very well matched, but the S_{11} is lower than -6 dB around 600 MHz, and an additional matching system can be used to improve S_{11}. Nevertheless, even if the antenna is not perfectly matched, the mismatching level does not prevent the measurement of radiation patterns and gain.

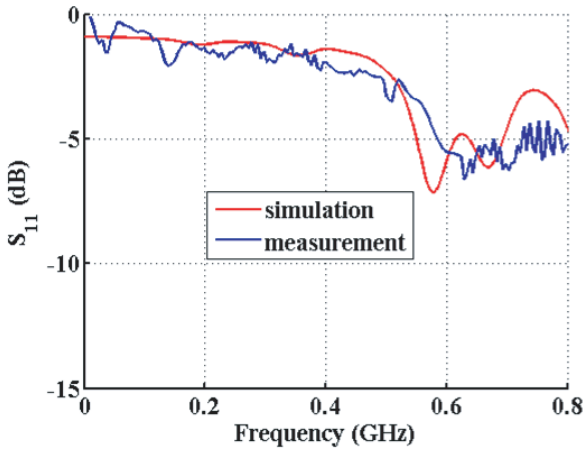

Figure 6. Simulated and measured S_{11} magnitude of the monopole without reflector plane.

The radiation patterns are presented for two cases: Without and with reflector plane to improve gain.

3.1. Antenna without Reflector

The radiation patterns of the monopole antenna without reflector are presented in this section. Fig. 7 shows the radiation patterns for simulation at 550 MHz and measurement at 490 MHz in the E- and H-planes, respectively. The simulated and measured results are quite similar. It is easy to see that in the E-plane, the antenna radiates more towards the opened side. In all cases, we observe a frequency shift between measurement and simulation due to the inadequate knowledge of exact plasma parameters.

The radiation patterns for simulation at 600 MHz and measurement at 540 MHz in the E- and H-planes respectively are presented in Fig. 8.

Figs. 7(b) and 8(b) show that the measured radiation patterns in H plane are not completely omnidirectional because for measurement the antenna is put on a pylon made from polyvinyl-chloride (PVC).

For the plasma OFF case and for all frequencies in simulation and measurement, the antenna gain is slightly decreased (under -25 dBi). The results show that when the plasma is OFF, the antenna does not radiate, can become furtive in a reception antenna case, and demonstrate that the feeding system does not radiate.

The simulated and measured maximum realized gains for our antenna system without reflector are shown in Table 1. We can notice that the gains in simulation and measurement are quite similar even if real plasma media induces loss because it cannot be considered like a perfect conductor.

From the gain, the efficiency of the antenna is evaluated and shown in Table 1. The radiating efficiency for the simulated frequencies is equal to 35.4% (550 MHz) and 47.1% (600 MHz) and for measured frequencies 26.9% (490 MHz) and 43.3% (540 MHz). The total efficiency with mismatching effect of the antenna is also shown in Table 1.

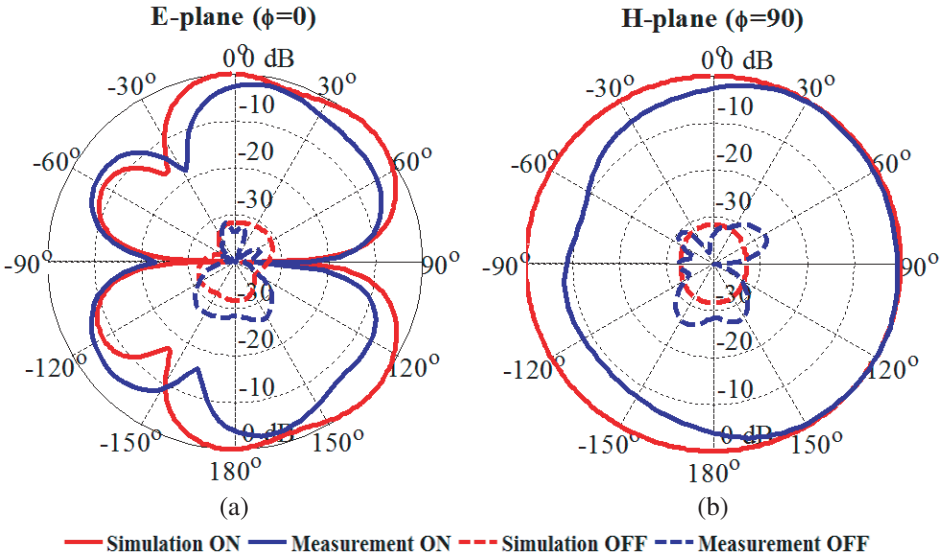

Figure 7. Normalized radiation patterns for the simulation at 550 MHz and measurement at 490 MHz of the monopole without reflector plane. (a) E-plane, E_θ component. (b) H-plane, E_ϕ component.

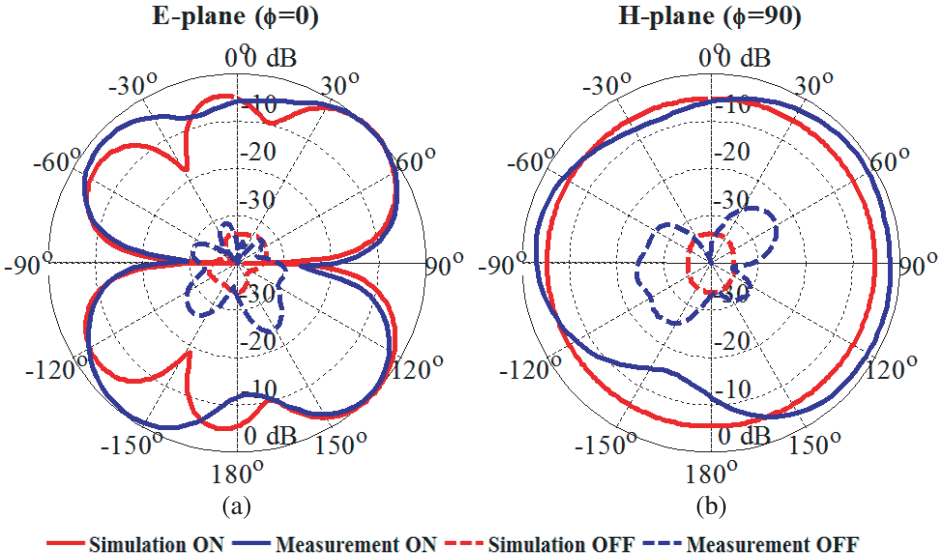

Figure 8. Normalized radiation patterns for the simulation at 600 MHz and measurement at 540 MHz of the monopole without reflector plane. (a) E-plane, E_θ component. (b) H-plane, E_ϕ component.

Table 1. Maximum realized gain and efficiency in simulation and measurement for the monopole without reflector.

	Simulated frequencies		**Measured frequencies**	
Frequency (MHz)	550	600	490	540
Gain plasma ON case (dBi)	−3.1	0.1	−4.3	−2.1
Gain plasma OFF case (dBi)	−34	−32	−29.7	−23.5
Radiated efficiency (%)	35.4	47.1	26.9	43.3
Total efficiency (%)	24.2	35	11.9	23

3.2. Antenna with Reflector

This section presents the radiation patterns of the antenna with reflector for only one distance $d = \lambda/4$ at 600 MHz.

Fig. 9 represents the simulated (at 550 MHz) and measured (at 490 MHz) radiation patterns in E and H-planes. The simulation and measurement are quite similar.

Fig. 10 shows the radiations patterns in simulation at 600 MHz and in measurement at 540 MHz for E and H-planes. The front to back ratio (f/b) is more than 10 dB.

The simulated and measured maximum realized gains for our antenna system with reflector are

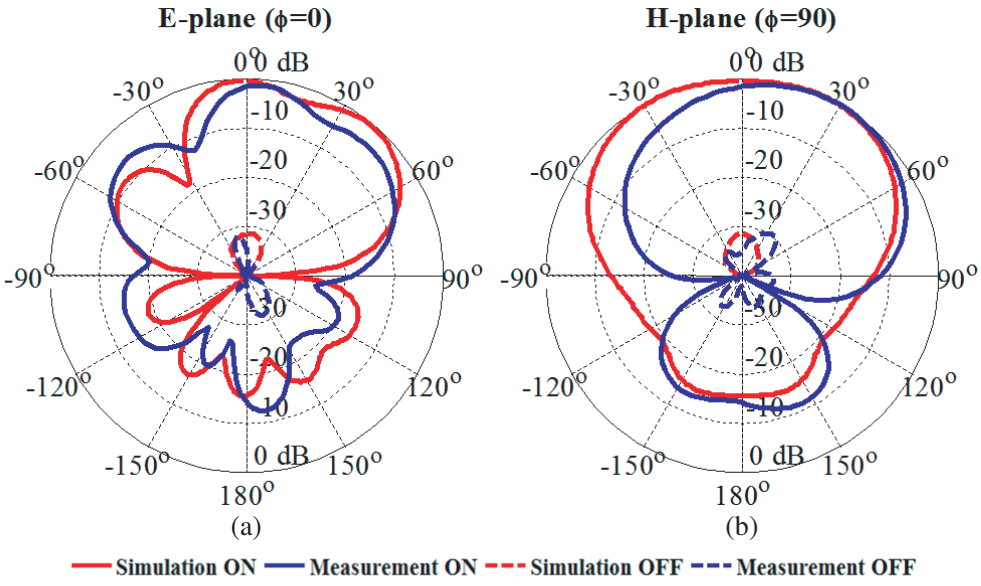

Figure 9. Normalized radiation patterns for the simulation at 550 MHz and measurement at 490 MHz of the monopole with reflector plane. (a) E-plane, E_θ component. (b) H-plane, E_ϕ component.

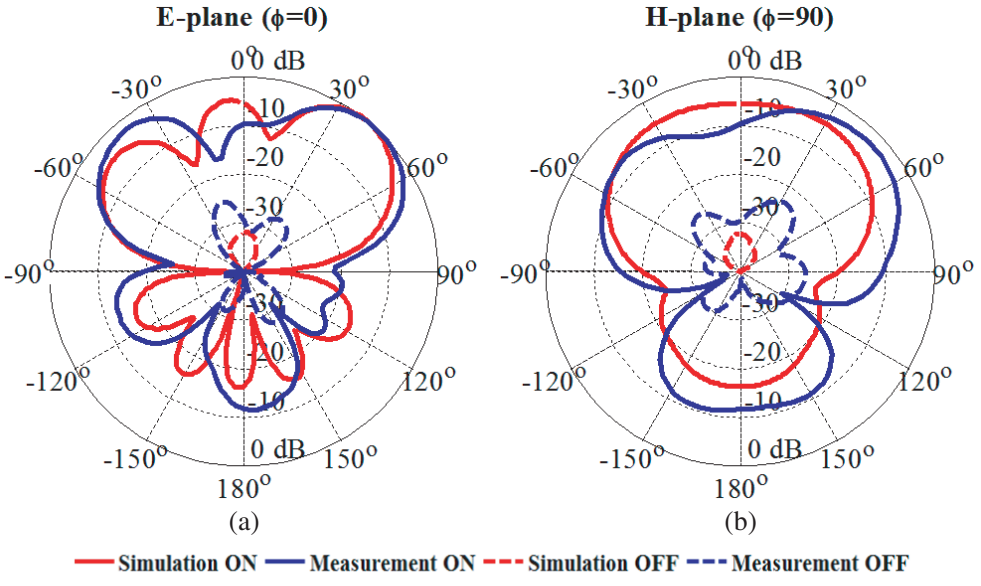

Figure 10. Normalized radiation patterns for the simulation at 600 MHz and measurement at 540 MHz of the monopole with reflector plane. (a) E-plane, E_θ component. (b) H-plane, E_ϕ component.

Table 2. Maximum realized gain in simulation and measurement for the monopole with reflector.

	Simulated frequencies		**Measured frequencies**	
Frequency (MHz)	550	600	490	540
Gain plasma ON case (dBi)	2.5	5	−0.3	1
Gain plasma OFF case (dBi)	−28.8	−27	−28	−22.1

shown in Table 2. The measurement and simulation are quite similar. It is important to note that the reflector plane increases the gain of 5 dB in simulation and 3 dB in measurement. At the measured frequency 540 MHz, a positive gain of 1 dB is obtained in the plasma ON case.

4. CONCLUSION

In this paper, a cylindrical plasma antenna working as monopole or dipole is presented and completely characterized in terms of radiation patterns and gain. A new feeding system is designed to couple electromagnetic signal from the input coaxial line to the plasma tube to be radiated. The simulated and measured results are in quite good agreement except the frequency shift of the antenna behavior. This defect could be improved by a better knowledge of the plasma parameters. From our knowledge, this antenna system is one of the first investigated monopole or dipole plasma antennas with measurement of radiation patterns and positive gain.

ACKNOWLEDGMENT

The authors would like to acknowledge Jean Christophe Lecun and Jérôme Sol from IETR for their technical support.

REFERENCES

1. Inan, U. S. and M. Golkowski, *Principles of Plasma Physics for Engineers and Scientists*, Cambridge University Press, New York, 2011.
2. Laroussi, M. and J. R. Roth, "Numerical calculation of the reflection, absorption, and transmission of microwaves by nonuniform plasma slab," *IEEE Trans. Plasma Sci.*, Vol. 21, 366–372, Aug. 1993.
3. Alexeff, I., T. Anderson, S. Parameswaran, E. P. Pradeep, J. Hulloli, and P. Hulloli, "Experimental and theoretical results with plasma antennas," *IEEE Trans. Plasma Sci.*, Vol. 34, No. 2, 166–172, Apr. 2006.
4. Anderson, T., "Smart plasma antenna," *Plasma Antennas*, 79–112, Artech House, MA, Norwood, 2011.
5. Zali, H. M., M. T. Ali, N. A. Halili, H. Ja'afar, and I. Pasya, "Study of monopole plasma antenna using fluorescent tube in wireless transmission experiments," *2012 International Symposium on Telecommunication Technologies (ISTT)*, 52–55, 2012.
6. W. Jiayin, S. Jiaming, W. Jiachun, and X. Bo, "Study of the radiation pattern of the unipole plasma antenna," *2006 7th International Symposium on Antennas, Propagation EM Theory*, 1–4, 2006.
7. Sun, J., Y. Xu, and H. Sun, "Experience on plasma antenna technology," *2015 Asia-Pacific Microwave Conference (APMC)*, Vol. 2, 1–3, 2015.
8. Zhao, J. S., Y. J. Li, S. J. Xu, J. Yao, Y. H. Zhang, and Z. T. Zhang, "Analysis on radiation characteristics and electromagnetic compatibility of 10 kHz AC plasma antenna," *High Voltage Eng.*, Vol. 38, No. 9, 2336–2342, 2012 (in Chinese).
9. Zhao, J., Y. Chen, Y. Sun, H. Wu, Y. Liu, and Q. Yuan, "Plasma antennas driven by 5–20 kHz AC power supply," *AIP Adv.*, Vol. 5, No. 12, 127114-1–127114-11, 2015.

10. Zali, H. M., M. T. Ali, N. A. Halili, H. Ja'afar, A. N. Dagang, and I. Pasya, "Design monopole antenna with florescent tube at 4.9 GHz," *Asia-Pacific Microwave Conference Proceedings*, 1049–1051, 2013.
11. Zhu, A., Z. Chen, and J. Lv, "Reconfigurable characteristics of the monopole plasma antenna and its array driven by surface wave," *WSEAS Transactions on Communication*, Vol. 12, No. 4, Apr. 2013.
12. Cerri, G., R. De Leo, V. M. Primiani, and P. Russo, "Measurement of the properties of a plasma column used as a radiated element," *IEEE Trans. on Instrumentation and Measurement*, Vol. 57, No. 2, 242–247, Feb. 2008.
13. Li, X. S., F. Luo, and B. J. Hu, "FDTD analysis of radiation performance of a cylinder plasma antenna," *IEEE Antennas Wireless Propag. Lett.*, Vol. 8, 756–758, 2009.
14. Ghaderi, M., G. Moradi, and P. Mousavi, "Numerical study on a wideband plasma folded-dipole antenna," *IEEE Antennas Wireless Propag. Lett.*, Vol. 16, 2017.
15. Badawy, M. M., H. A. E. A. Malhat, S. H. Zainud-Deen, and K. H. Awadalla, "a simple equivalent circuit model for plasma dipole antenna," *IEEE Transactions on Plasma Science*, Vol. 43, No. 12, 4092–4098, Dec. 2015.
16. CST, "Computer Simulation Technology," http://www.cst.com/.
17. Jusoh, M. T., M. Himdi, F. Colombel, and O. Lafond, "Performance and radiation patterns of a reconfigurable plasma corner-reflector antenna," *IEEE Antennas and Wireless Propagation Letters*, No. 99, 1137–1140, 2013.
18. Lebbar, H., M. Himdi, and J. P. Daniel, "Transmission line analysis of printed monopole," *Electronics Letters*, Vol. 28, No. 14, 1326–1327, Jul. 1992.
19. Akan, V. and E. Yazgan, "Analysis of the relation between printed strip monopole and dielectric coated thin cylindrical monopole," *2010 10th Mediterranean Microwave Symposium*, 77–80, 2010.